

Static impurities in the $S = 3/2$ kagome lattice

A. Läuchli and S. Dommange*

*Institut Romand de Recherche Numérique en Physique des Matériaux
(IRRMA), PPH-Ecublens, CH-1015 Lausanne, Switzerland*

B. Normand

*Département de Physique, Université de Fribourg, CH-1700 Fribourg, Switzerland and
Theoretische Physik, ETH-Hönggerberg, CH-8093 Zürich, Switzerland*

F. Mila

*Institute of Theoretical Physics, Ecole Polytechnique Fédérale de Lausanne, CH-1015 Lausanne, Switzerland
(Dated: November 30, 2018)*

We consider the effects of doping the $S = 3/2$ kagome lattice with static, nonmagnetic impurities. By exact-diagonalization calculations on small clusters we deduce the local spin correlations and magnetization distribution around a vacancy. As in the $S = 1/2$ kagome lattice, in the vicinity of the impurity we find an extended region where the spin correlations are altered as a consequence of frustration relief, and no indications for the formation of local moments. We discuss the implications of our results for local-probe measurements on $S = 3/2$ kagome materials.

PACS numbers: 75.10.Jm, 75.30.Hx, 76.60.-k

I. INTRODUCTION

The kagome antiferromagnet (Fig. 1) is one of the most highly frustrated geometries known in two-dimensional (2d) systems with only nearest-neighbor interactions, for both classical and quantum spins. A variety of materials displaying the kagome structure is known to exist, and their number continues to increase. Because of the long-standing absence of a true $S = 1/2$ kagome spin system, the majority of experimental studies of quantum kagome antiferromagnets has focused on compounds with higher spins. These include the jarosites $(\text{H}_3\text{O})\text{Fe}_3(\text{OH})_6(\text{SO}_4)_2$,¹ and $\text{KFe}_3(\text{OH})_6(\text{SO}_4)_2$, both $S = 5/2$, and $\text{KCr}_3(\text{OH})_6(\text{SO}_4)_2$,^{2,3} which has $S = 3/2$. In the magnetoplumbite $\text{SrCr}_9\text{pGa}_{12-9\text{p}}\text{O}_{19}$ (SCGO),⁴ most of the $S = 3/2$ Cr^{3+} ions form kagome bilayer units with frustrated interlayer coupling. The related compound $\text{Ba}_2\text{Sn}_2\text{ZnCr}_{7\text{p}}\text{Ga}_{10-7\text{p}}\text{O}_{22}$ (BSZCGO)⁵ contains the same units with a superior interbilayer separation and a lower intrinsic impurity concentration. In both of the latter materials, ideal stoichiometry ($p = 1$) remains unachievable, making the influence of static (and for Ga^{3+} spinless) impurities an important factor determining the physical response.

The very recent synthesis of the $S = 1/2$ kagome compound $\text{ZnCu}_3(\text{OH})_6\text{Cl}_2$ ⁶ makes a detailed comparison of these different systems indispensable. Among the local-probe techniques which have been refined for specific studies of impurities in spin systems, nuclear magnetic resonance (NMR)^{7,8,9,10} and muon spin resonance (μSR)^{9,11} experiments have provided the most valuable information obtained to date. Inelastic neutron scattering measurements offer additional insight into the excitations of the bulk system, suggesting an exotic, gapless spin-liquid state for $\text{ZnCu}_3(\text{OH})_6\text{Cl}_2$ ($S = 1/2$)¹² and a rather conventional spin-wave spec-

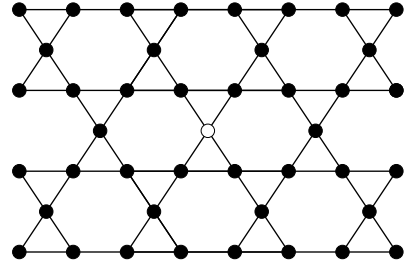


FIG. 1: The kagome lattice. The central site has been replaced by a nonmagnetic impurity.

trum with a quasi-flat band for $\text{KFe}_3(\text{OH})_6(\text{SO}_4)_2$ ($S = 5/2$),¹³ where Dzyaloshinskii-Moriya interactions have a significant role.

On the theoretical level, studies of the classical kagome antiferromagnet are complicated by the infinite ground-state degeneracy. For quantum spin systems, the $S = 1/2$ kagome lattice has been shown to have a spin-liquid ground state,¹⁴ with an exceptionally short spin-spin correlation length of 1.3 lattice constants.^{15,16} The excitation spectrum¹⁷ is dominated by an exponentially large number of low-lying singlets.¹⁸ Both ground and singlet excited states are found to be very well described by a resonating-valence-bond (RVB) framework based only on the manifold of nearest-neighbor dimer coverings.¹⁹

By contrast, the situation for the $S = 3/2$ system has been the subject of rather less attention. An early spin-wave analysis²⁰ suggested that it may support long-ranged antiferromagnetic order, but a large- N approach²¹ was found to favor a quantum-disordered state with the same properties (including a triplet gap and deconfined spinon excitations) as predicted for the $S = 1/2$ system. Preliminary numerical results²² for the

$S = 3/2$ system are complex and difficult to interpret, making it not yet possible to give an unambiguous statement on the underlying physics of this system: there is no specific evidence either for an ordered state or for a valence–bond description, and while the excitation spectrum shows certain parallels to the $S = 1/2$ case, there are no indications for either spin waves or spinons.

Studies of static vacancies in spin liquids and gapped quantum magnets have been used in a number of systems to obtain additional information concerning spin correlations, and occasionally to reveal novel phenomena. The only investigations performed to date for kagome antiferromagnets have addressed the two limits, namely the maximally quantum and the purely classical. For the $S = 1/2$ system it was shown in Ref. 23 that nonmagnetic impurities do not generate free spin degrees of freedom in their vicinity, that they lower the number of low-lying singlet states, induce interdimer correlations over a significant range despite the very short spin correlation length, and experience a highly unconventional mutual repulsion; much of this exotic behavior is also contained within the RVB description. For the classical system, it was shown in Ref. 24 that site disorder competes with thermal selection to favor states where frustration relief takes the form of noncoplanar spin configurations around the impurity site. Similar ideas were also articulated in Ref. 25.

In this study we investigate the effects of static impurities in the $S = 3/2$ kagome lattice with a view to offering a sound basis for the interpretation of experimental results. We will show that, as in the $S = 1/2$ system, spin correlations are modified over a significant number of bonds at different distances from the impurity site, and that there is no evidence for free local moments induced around these sites. We provide a brief and qualitative motivation for these phenomena in terms of changes in the spin correlations analogous to the local collinearity enhancement of classical spins due to the relief of frustration at an impurity.

In Sec. II we consider the spin–spin correlations on all bonds in the presence of an impurity in a $S = 3/2$ kagome cluster. Section III presents the local magnetization distribution around an impurity site, which we compute for all spin sectors. In Sec. IV we discuss the extent to which our results may assist in the interpretation of NMR, μ SR and other measurements on the $S = 3/2$ kagome systems now under experimental investigation. Section V summarizes our conclusions.

II. SPIN CORRELATIONS

A. Exact Diagonalization

We perform exact–diagonalization (ED) calculations for the Heisenberg Hamiltonian

$$H = J \sum_{\langle ij \rangle} \mathbf{S}_i \cdot \mathbf{S}_j, \quad (1)$$

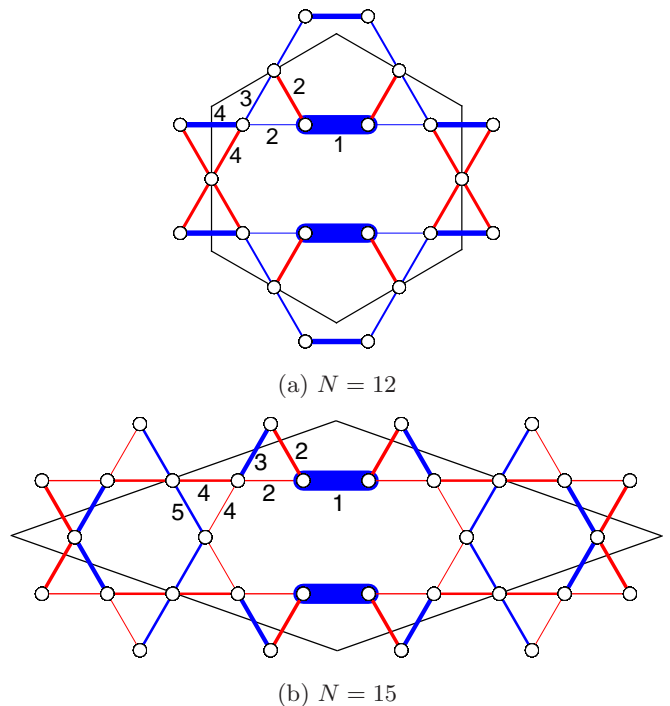


FIG. 2: Bond spin–spin correlations for a single impurity in 12- and 15-site clusters, obtained by ED. Bar width represents the strength of correlation functions on each bond, measured as a deviation from the pure–system values $C_0(12) = E_g(12)/J = -1.463$ and $C_0(15) = E_g(15)/J = -1.448$, on a linear scale where the strongest correlation function is $\langle \mathbf{S}_i \cdot \mathbf{S}_j \rangle = -2.994$. Blue (red) lines denote bonds on which the deviation is negative (positive). The black lines denote the boundaries of the cluster.

where J is the antiferromagnetic superexchange interaction and $\langle ij \rangle$ denotes nearest–neighbor sites, for small clusters of $S = 3/2$ spins with periodic boundary conditions. Because of the large Hilbert spaces required when dealing with spins $S > 1/2$, the cluster size is restricted to a maximum of 15 sites with one impurity. We compute the total energy, the bond spin–spin correlation functions $C_{ij} = \langle \mathbf{S}_i \cdot \mathbf{S}_j \rangle$ for all nearest–neighbor pairs $\langle ij \rangle$ and the induced magnetizations on each site in every spin sector.

Specifically, we have studied standard kagome clusters of 12 and 15 sites in which one $S = 3/2$ spin is replaced by a nonmagnetic impurity. In the 12-site clusters all sites are equivalent before dilution, whereas in the 15-site case there are two types of site which are inequivalent under the symmetries of the cluster. We have verified that our conclusions do not depend on choice of the dilution site. We note here that the ground state of the diluted 12-site system has total spin $S = 1/2$, while the diluted 15-site cluster has a singlet ground state.

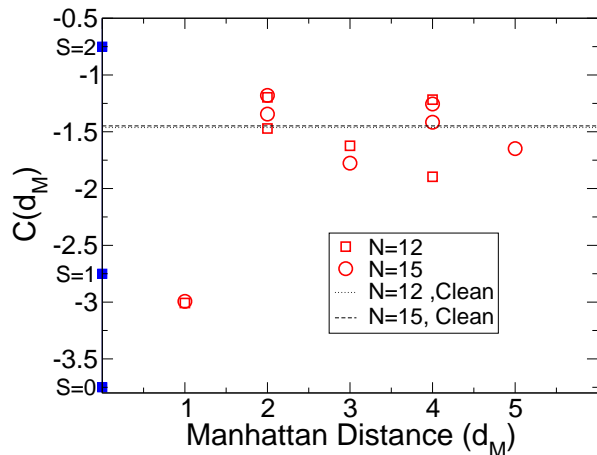


FIG. 3: Bond spin–spin correlation functions $C(d_M) = \langle \mathbf{S}_i \cdot \mathbf{S}_j \rangle$ on nearest–neighbor bonds as a function of their Manhattan distance d_M from a single impurity, for clusters of 12 and 15 sites. The site–bond separation d_M corresponds to the site labels shown in Fig. 2. The dotted and dashed lines show the value of $\langle \mathbf{S}_i \cdot \mathbf{S}_j \rangle$ for impurity–free systems of sizes $N = 12$ and $N = 15$, and are almost indistinguishable.

B. Spin–spin correlation function

The bond spin–spin correlation functions C_{ij} around a single impurity are shown in Fig. 2. It is clear that spin correlations are strengthened on the bonds neighboring the vacant site. For a quantitative measure of this effect, we remind the reader that the spin correlation, or Heisenberg energy per bond $E = J\mathbf{S}_i \cdot \mathbf{S}_j$, takes the values $E_0 = -15J/4$ if the two spins form a pure singlet, $E_1 = -11J/4$ for a triplet, $E_2 = -3J/4$ for a quintet, and $E_3 = 9J/4$ for a heptet state. The pure–system results $E_g(N = 12) = -1.463J$ and $E_g(N = 15) = -1.448J$ per bond are used to set the positive and negative values shown in Fig. 2, and also represent the average extent to which the bonds are dissatisfied (frustrated) in the $S = 3/2$ kagome antiferromagnet.

The strengthening of correlations is manifestly not as strong as in the $S = 1/2$ case, and the system remains far from perfect singlet formation on the nearest–neighbor bonds. For $S=3/2$, the correlation on the strongest bond near the impurity (number 1 in Fig.2) represents 80% of the maximal (negative) possible value, and the next one (number 3 in Fig.2) 47% for the 15-site cluster, to be compared with 92% and 70% for the $S=1/2$ case (taken from Ref. 23 for 27 sites).

The most straightforward interpretation of the strengthening of correlations is that the two spins on each bond attain a more antiferromagnetic state as a consequence of the relief of frustration in their triangle²⁶ caused by the removal of the apical site; this effect was represented as an enhancement of collinearity for classical spins in Ref. 24. A corollary of this enhancement is the weakening of spin correlations on next–nearest–neighbor bonds. A certain oscillatory behavior of the

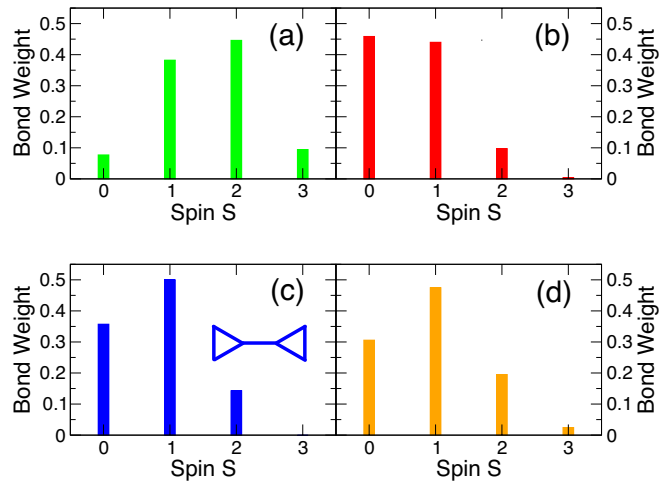


FIG. 4: Distribution of bond spin states obtained from ED calculations on the $S = 3/2$ kagome antiferromagnet for (a) a bond far from an impurity, computed for an undoped 12–site cluster, (b) a bond next to an impurity, obtained from a 15–site cluster, and (c) the central bond of the 6–site cluster shown in the inset. In panel (d) is shown the analogous bond distribution for an undoped $S = 3/2$ square lattice.

spin correlations is discernible in the values C_{ij} as the separation of the bond from the impurity is increased, as shown in Fig. 3. Although this appears neither as strong nor as long–ranged as in the $S = 1/2$ case, the effect clearly extends well beyond the nearest–neighbor sites. Unlike the $S = 1/2$ case, these spin correlations do not illustrate directly the absence of local moments, which we demonstrate in Sec. III. While the size of the cluster sets an obvious limit on the strength of these statements, we may conclude that impurity doping causes a disruption of the pure–system spin configuration which is not entirely local, and induces at least short–ranged dimer correlations with a characteristic length of several lattice constants.

C. Bond spin correlations

Further insight into the nature of the spin correlations and their alteration in the presence of impurities may be gleaned from the weights of the 4 possible spin states present on a given bond, which are shown in Figs. 4(a–d). For a bond far from an impurity site [Fig. 4(a)], one observes that this weight distribution is approximately symmetrical, with the majority of bonds in states of total spin 1 or 2, while the probability for a bond to be a perfect singlet or fully spin–polarized is small. Figure 4(b) shows the situation for a bond next to an impurity site, where there is a very significant shift of weight away from high–spin states, particularly $S = 2$, to the net singlet state. This result quantifies the quantum analog of the classical collinearity enhancement, although as noted in the previous section this is by no means as overwhelmingly

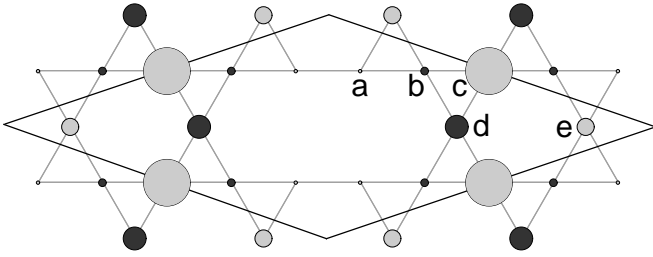


FIG. 5: Site magnetization profile of the lowest triplet state induced by a single impurity in a 15-site cluster. Circle radius represents the magnitude of the local moment on a linear scale where the largest circle corresponds to a moment of $0.722\mu_B$ ($0.5\mu_B$ is the moment of a free electron), and the dark grey circles represent sites with induced moments opposite to the effective field direction. The black lines denote the boundary of the cluster.

strong as in the $S = 1/2$ system. In Fig. 4(c) the same distribution is presented for the central bond of the 6-site cluster shown in the inset, which has $\langle \mathbf{S}_i \cdot \mathbf{S}_j \rangle = -2.821$. From the similarity to Fig. 4(b) one may conclude that the physical processes contributing to the spin correlations on the bond with relieved frustration are largely local in nature.

For further comparison, in Fig. 4(d) we show the same distribution calculated for a square lattice of spins $S = 3/2$ with no impurities. If this distribution is considered to be representative of the situation in an unfrustrated, collinear 2d system, a comparison with Fig. 4(a), where the highest weight is found for bonds of spin 2, shows the effects of the frustrated kagome geometry in driving the system away from a satisfied antiferromagnetic state. From the bond spin distributions (Fig. 4) one may also comment on the suitability of a description for the $S = 3/2$ kagome system based on local singlet formation. While this type of framework was used with considerable success in the $S = 1/2$ case, it is clear immediately from Fig. 4(a), where over 80% of the bonds in the pure system have spin states $S = 1$ and 2, that a basis of local bond singlets would not be expected to capture the dominant physics in this case.

III. INDUCED MAGNETIZATION

The local magnetization pattern induced in the vicinity of a doped nonmagnetic impurity is computed in the ED technique by considering for example the sector of total spin $(S, S_z) = (1, 1)$, and is shown for a 15-site cluster in Fig. 5. The site magnetizations are to some extent anticorrelated with the deviation of C_{ij} from C_0 shown in Figs. 2 and 3. The most obvious feature is the absence of local moments induced on the sites directly neighboring the impurity, a feature in common with the $S = 1/2$ system but in contrast to the majority of gapped quan-

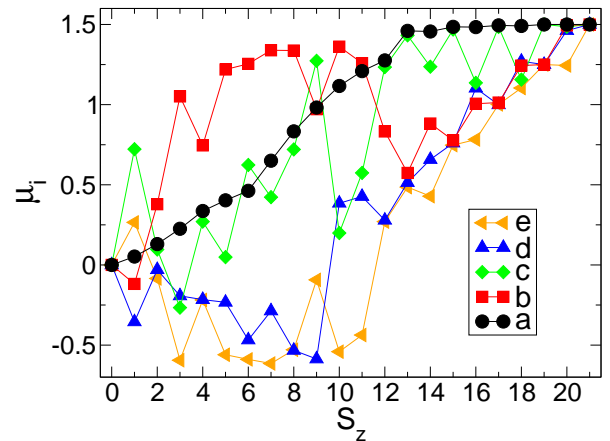


FIG. 6: Induced magnetization per site μ_i as a function of the spin sector S_z for all inequivalent sites neighboring an impurity, computed by ED for a 15-site cluster. The site labels correspond to those shown in Fig. 5.

tum magnets considered in this context. The induced moments are strongest on the sites most distant from the impurity, also suggesting, as in the $S = 1/2$ case, a phenomenon of longer range where the moments would be found further from the impurity on a larger cluster. Such an extended magnetization profile is suggested by NMR and μ SR measurements performed on SCGO and BSZCGO^{7,8,11} (Sec. IV).

The magnetization induced on each site by a nonmagnetic impurity is shown in Fig. 6 for all of the spin sectors obtainable on a 15-site cluster. The spin sector may be considered to reflect the state of the system under an applied magnetic field which changes the magnetisation from zero ($S_z = 0$) to saturation ($S_z = 21$). Unlike the $S = 1/2$ case there is no apparent “protection” of the nearest-neighbor sites (filled circles in Fig. 6), reflecting the fact that these are not bound into perfect dimers. The immediate polarization of the moment on these sites with the effective field is to be expected from the fact that the bond spin state is primarily a superposition of singlets and triplets [Fig. 4(b)]. The magnetization at these sites increases linearly to a local saturation at rather less than $2/3$ of the total saturation, as a consequence of their lower connectivity. The more distant sites show a complex and non-monotonic evolution of their local moments which suggests a rearrangement of the induced magnetization with applied field, and presumably strong effects of the finite cluster size in the calculation.

IV. DISCUSSION

NMR and μ SR are the techniques of choice for measuring in real space the effects of doped impurities on magnetizations and spin correlations. In NMR it is the shifts, linewidth alterations and on occasion relaxation times which yield information concerning these quanti-

ties. In μ SR it is the temperature-, field-, and doping-dependence of the muon relaxation time, the last being the most instructive with regard to the spatial extent of the spin excitations responsible for relaxation. The diluted $S = 3/2$ kagome bilayer systems SCGO and BSZCGO have been the subject of an extensive program of investigation. It goes back to an early investigation of SCGO with μ SR²⁷ which opened the way to more recent μ SR investigations²⁸. The most recent detailed results including both NMR and μ SR are contained in Refs. 7, 8, and 11, and are summarized in Refs. 29 and 30. Both materials have intrinsic doping of Cr^{3+} sites by nonmagnetic Ga^{3+} ions in the kagome bilayers, in quantities exceeding 5% and 3% respectively, although in BSZCGO there is evidence for a second type of defect state possibly related to Zn impurities. NMR studies including NQR (nuclear quadrupole resonance) measurements were performed on ^{71}Ga sites in SCGO and BSZCGO, accompanied by μ SR experiments on both materials.

We abstract the primary features observed in experiment, and compare these to the results of the calculations presented in Secs. II and III. We focus only on qualitative behavior, as a quantitative determination of any physical properties (shifts, line widths, relaxation rates) would require a specific Hamiltonian for local and hyperfine interactions. We caution the reader also that our calculations do not include the possibility of additional interactions breaking SU(2) spin symmetry on each bond; in particular the Dzyaloshinskii–Moriya interactions which may be present in these low-symmetry crystal structures are known to have a very significant effect on local magnetizations (Sec. III)³¹.

Both experimental techniques find no evidence for a singlet–triplet gap at temperatures down to 30 mK, which is consistent with the presence of all types of states at low energies on a finite cluster. The line shape observed in NMR shift measurements indicates the presence of many inequivalent sites, consistent with the large spatial extent of the region affected by a single impurity. The extended nature of the perturbation is also reflected in symmetric line shapes. The density of very low-energy spin excitations is manifest in μ SR experiments as the observation of “quantum dynamics” persisting as $T \rightarrow 0$. The spatial extent of these collective (as opposed to local) spin fluctuations is reflected both in the doping-dependence of the relaxation rate and directly in the relaxation of muons at sites far from any impurities.

The important qualitative features of both the experiments and the numerical calculations are the absence of a single spin degree of freedom anywhere in the vicinity of the impurity, and the rather large extent of the area of affected sites in spite of the very short spin correlation lengths. We stress that these features, which are common to both $S = 1/2$ ²³ and $S = 3/2$, are common because of the highly frustrated kagome geometry: as noted in Secs. I–III there is currently little evidence for a common description of the two systems. For the $S =$

$3/2$ Heisenberg model on the kagome lattice, a very small or vanishing spin gap and the near-degeneracy of considerable numbers of basis states are sufficient to yield the results we have obtained. There is as yet no framework providing an unambiguous understanding of the nature of the pure system, by which is meant providing ground and excited states satisfying these criteria, and it has been possible only to exclude some candidate descriptions, such as a discernible magnetic order or an origin in formation of local singlets. To date there is also no evidence for the possibility of deconfined, spinon-like excitations of the type sometimes invoked in the discussion of the $S = 1/2$ system.

We reiterate that, as already shown for the $S = 1/2$ case, kagome systems do not form part of the paradigm obeyed by many unfrustrated low-dimensional spin systems in which a local moment is formed near a doped vacancy. Instead, an extended envelope of weak magnetization is induced over a considerable range, and is maximal some distance from the impurity site. Despite the antiferromagnetic spin correlations, in kagome systems there is no sense in which the induced magnetization, or spin polarization, can be said to be staggered; this result is also common to the $S = 1/2$ case,²³ and is a consequence of the strongly frustrated geometry. An alternation is, however, found in the bond spin correlation functions, corresponding to an induced dimer–dimer correlation with a range of several lattice constants.

V. SUMMARY

We have investigated the effects of static, spinless impurities doped into the $S = 3/2$ antiferromagnetic Heisenberg model on the kagome lattice. By analysis of spin–spin correlation functions and of the induced local magnetization, we find that nonmagnetic impurities in the kagome lattice have the important property that they do not generate localized spins at the vacant site, and do have an extended range of influence on the correlated spin background. Unlike the $S = 1/2$ case, where the development of dimer correlations over significant distances could be considered as due to a hole-induced freezing of singlet resonances,²³ here it appears more appropriate to consider the phenomenon more generally as the result of enhanced local collinearity due to frustration relief.

Our results are in excellent agreement with all of the qualitative features observed in local-probe experiments. This constitutes an important contribution to the definition of a set of generic properties of the doped kagome system. It also indicates that the materials SCGO and BSZCGO, despite their bilayer geometry, do share these kagome hallmarks. Because these systems do not have complete filling of the kagome lattice sites by $S = 3/2$ ions, the study of impurity effects is a significant component of their characterization.

We close by reminding the reader that the results we have presented are obtained for very small systems, and

thus while indicative they cannot be considered as definitive. They should be regarded as provisional also in the sense that the ground state and nature of spin correlations in the $S = 3/2$ kagome antiferromagnet remain poorly characterized. However, they are sufficient to illustrate the general features which lie at the origin of the observed behavior in this system.

Acknowledgments

We are grateful to P. Mendels for valuable discussions. This work was supported by the Swiss National Science Foundation, both directly and through its MaNEP project.

-
- * deceased
- ¹ A. S. Wills, A. Harrison, C. Ritter, and R. I. Smith, *Phys. Rev. B* **61**, 6156 (2000).
 - ² A. Keren, K. Kojima, L. P. Le, G. M. Luke, W. D. Wu, Y. J. Uemura, M. Takano, H. Dabkowska, and M. J. P. Gingras, *Phys. Rev. B* **53**, 6451 (1996).
 - ³ S.-H. Lee, C. Broholm, M. F. Collins, L. Heller, A. P. Ramirez, Ch. Kloc, E. Bucher, R. W. Erwin, and N. Laceric, *Phys. Rev. B* **56**, 8091 (1997).
 - ⁴ X. Obradors, A. Labarta, A. Isalgué, J. Tejada, J. Rodriguez, and M. Pernet, *Solid State Commun.* **65**, 189 (1988).
 - ⁵ I. S. Hagemann, Q. Huang, X. P. A. Gao, A. P. Ramirez, and R. J. Cava, *Phys. Rev. Lett.* **86**, 894 (2001).
 - ⁶ M. P. Shores, E. A. Nytko, B. M. Barlett, and D. G. Nocera, *J. Am. Chem. Soc.* **127**, 13462 (2005).
 - ⁷ L. Limot, P. Mendels, G. Collin, C. Mondelli, B. Ouladdiaf, H. Mutka, N. Blanchard, and M. Mekata, *Phys. Rev. B* **65**, 144447 (2002).
 - ⁸ D. Bono, P. Mendels, G. Collin, and N. Blanchard, *Phys. Rev. Lett.* **92**, 217202 (2004).
 - ⁹ O. Ofer, A. Keren, E. A. Nytko, M. P. Shores, B. M. Barlett, D. G. Nocera, C. Baines, and A. Amato, unpublished (cond-mat/0610540).
 - ¹⁰ T. Imai, E. A. Nytko, B. M. Barlett, M. P. Shores, and D. G. Nocera, unpublished (cond-mat/0703141).
 - ¹¹ D. Bono, P. Mendels, G. Collin, N. Blanchard, F. Bert, A. Amato, C. Baines, and A. D. Hillier, *Phys. Rev. Lett.* **93**, 187201 (2004).
 - ¹² J. S. Helton, K. Matan, M. P. Shores, E. A. Nytko, B. M. Barlett, Y. Yoshida, Y. Takano, A. Suslov, Y. Qiu, J.-H. Chung, D. G. Nocera, and Y. S. Lee, *Phys. Rev. Lett.* **98**, 107204 (2007).
 - ¹³ K. Matan, D. Grohol, D. G. Nocera, T. Yildirim, A. B. Harris, S. H. Lee, S. Nagler, and Y. S. Lee, *Phys. Rev. Lett.* **96**, 247201 (2006).
 - ¹⁴ J. T. Chalker and J. F. Eastmond, *Phys. Rev. B* **46**, 14 201 (1992).
 - ¹⁵ P. W. Leung and V. Elser, *Phys. Rev. B* **47**, 5459 (1993).
 - ¹⁶ C. Zeng and V. Elser, *Phys. Rev. B* **51**, 8318 (1995).
 - ¹⁷ P. Lecheminant, B. Bernu, C. Lhuillier, L. Pierre, and P. Sindzingre, *Phys. Rev. B* **56**, 2521 (1997); C. Waldtmann, H.-U. Everts, B. Bernu, C. Lhuillier, P. Sindzingre, P. Lecheminant, and L. Pierre, *Eur. Phys. J. B* **2**, 501 (1998).
 - ¹⁸ F. Mila, *Phys. Rev. Lett.* **81**, 2356 (1998).
 - ¹⁹ M. Mambrini and F. Mila, *Eur. Phys. J. B* **17**, 651 (2000).
 - ²⁰ A. Chubukov, *Phys. Rev. Lett.* **69**, 832 (1992).
 - ²¹ S. Sachdev, *Phys. Rev. B* **45**, 12377 (1992).
 - ²² A. Läuchli, S. Dommange, J.-B. Fouet, and F. Mila, unpublished.
 - ²³ S. Dommange, M. Mambrini, B. Normand, and F. Mila, *Phys. Rev. B* **68**, 224416 (2003).
 - ²⁴ E. F. Shender, V. B. Cherepanov, P. C. W. Holdsworth, and A. J. Berlinsky, *Phys. Rev. Lett.* **70**, 3812 (1993).
 - ²⁵ C. L. Henley, *Phys. Rev. Lett.* **62**, 2056 (1989); *Can. J. Phys.* **79**, 1307 (2001).
 - ²⁶ V. Elser, *Phys. Rev. Lett.* **62**, 2405 (1989).
 - ²⁷ Y. J. Uemura, A. Keren, K. Kojima, L. P. Le, G. M. Luke, W. D. Wu, Y. Ajiro, T. Asan2, Y. Kuriyama, M. Mekata, H. Kikuchi, and K. Kakurai, *Phys. Rev. Lett.* **73**, 3306(1994).
 - ²⁸ P. Mendels, A. Keren, L. Limot, M. Mekata, G. Collin, and M. Horvatic, *Phys. Rev. Lett.* **85**, 3496 (2000).
 - ²⁹ D. Bono, L. Limot, P. Mendels, G. Collin, and N. Blanchard, *Low Temp. Phys.* **31**, 704 (2005).
 - ³⁰ P. Mendels, A. Olariu, F. Bert, D. Bono, L. Limot, G. Collin, B. Ueland, P. Schiffer, R. J. Cava, N. Blanchard, F. Duc, J. C. Trombe, *J. Phys.: Condens. Matter* **19**, 145224 (2007).
 - ³¹ K. Kodama, S. Miyahara, M. Takigawa, M. Horvatic, C. Berthier, F. Mila, H. Kageyama, and Y. Ueda, *J. Phys. Condens. Matter* **17**, 61 (2005); M. Clemency, H. Mayaffre, C. Berthier, M. Horvatic, J.-B. Fouet, S. Miyahara, F. Mila, B. Chiari, and O. Piovesana, *Phys. Rev. Lett.* **97**, 167204 (2006); S. Miyahara, J.-B. Fouet, S. Manmana, R. Noack, H. Mayaffre, I. Sheikin, C. Berthier, and F. Mila, *Phys. Rev. B* **75**, 184402 (2007).